X-Ray Diffraction

ismisebrendan

October 24, 2023

Abstract

The lattice constants for NaCl, LiF, GaP and Si were measured through x-ray diffraction of crystals of NaCl(100), LiF(100), GaP(111), Si(100) and Si(111). The values obtained, $a_{NaCl} = 5.7 \pm 0.4$ Å, $a_{LiF} = 4.0 \pm 0.3$ Å, $a_{GaP} = 5.5 \pm 0.5$ Å and $a_{Si} = 5.3 \pm 0.6$ Å are all consistent with the literature values, albeit a bit imprecise. The diffraction pattern obtained for the Si(100) crystal is odd in that certain low-order peaks appear only for one orientation of the crystal. This affected the accuracy of the value obtained for a_{Si}. The accuracy and precision of this may be further improved through measurement at higher angular and time frequencies.

1 Introduction

Crystals are solids with a periodic pattern in 3D space. The crystal is made up of a 3D lattice of identical points. The lattice is defined by three non-coplanar basis vectors, $\vec{a}$, $\vec{b}$ and, $\vec{c}$, through linear combinations of which the entire lattice can be generated. The vectors $\vec{a}$, $\vec{b}$ and, $\vec{c}$ and the angles between them, γ, β and α, make up the unit cell, the basic constituent of any crystal lattice. In this experiment we are only concerned with cubic structures and so $|\vec{a}| = |\vec{b}| = |\vec{c}|$ and the three vectors are mutually orthogonal with $|\vec{a}| = a$ being known as the lattice constant. Multiple atoms can be assigned to the one lattice point and the selection of atoms which when assigned to the point can make up the entire crystal is known as the basis.[1],[2]

Sets of equally spaced parallel lattice planes separated by a distance d can be defined within a crystal lattice. In each set each plane has the same density of points. The planes are identified by their intercepts with the basis vectors of the lattice. If a plane has intercepts $\frac{a}{h}$, $\frac{b}{k}$ and $\frac{c}{l}$ then it is denoted by (hkl) where h, k and l are known as Miller indices. If the plane is perpendicular to one or more basis vectors it has an intercept at infinity and the corresponding Miller index is 0. In cases of cubic symmetry planes can be equivalent, such as the (100), (010) and (001) planes, all of which are related through symmetry.[1]

There are many different structures a crystal can have, however in this experiment we are only concerned with two types, the NaCl structure and the diamond/zinc blende (ZnS) structure. The NaCl or face-centred cubic structure is very common in ionic crystals with a 1:1 ratio of cations to anions with each ion being surrounded by six ions of the other element. This is the structure of LiF also.[3] The diamond structure is made up of one carbon atom (or any other suitable atom) covalently bonded to four others in a tetrahedral shape. This differs from the ZnS structure only in that in the ZnS structure half of the atoms are Zn and the other half are S (or any other suitable combination of atoms). Si takes on the diamond structure, while GaP takes on the ZnS structure. These structures are shown in figure 1.[4][5]

An x-ray spectrum produced in a lab is continuous (known as bremsstrahlung), starting from the short wavelength limit, rising rapidly to a maximum and then decreasing gradually with the intensity depending on the tube voltage. Superimposed on this is the characteristic spectrum of the target metal, in this case molybdenum (Mo).[2],[6]

This characteristic spectrum is made of sharp intensity maxima at certain wavelengths characteristic of the target metal. These maxima are grouped into sets of increasing wavelength labelled K, L, M, etc. Only the K lines are useful in x-ray diffraction as longer wavelengths are absorbed more easily in crystals. The characteristic spectrum arises from the incident electrons removing low energy electrons from the n = 1, 2, 3, etc. energy levels of the target atom. An outer electron then falls to fill the vacancy in that shell and loses energy as a photon of characteristic wavelength in the process. The K set is divided into Kα and Kβ lines. Kα lines arise from electrons in the L shell falling to the K shell, and Kβ lines are due to electrons falling to the K shell from the M shell. The Kα line (it is actually a doublet, however they are often not resolved separately) is more

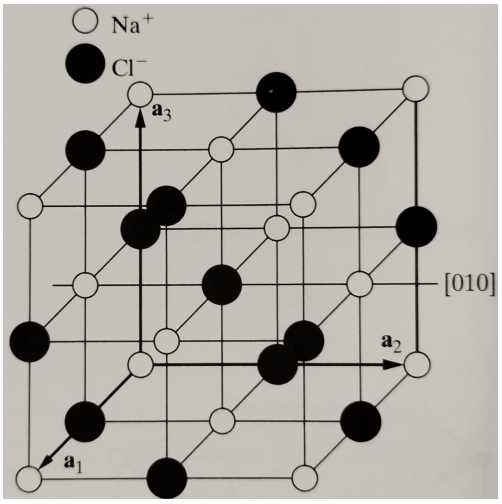

(a) The NaCl structure. The filled in circles represent the anions while the empty circles represent the cations.[2]

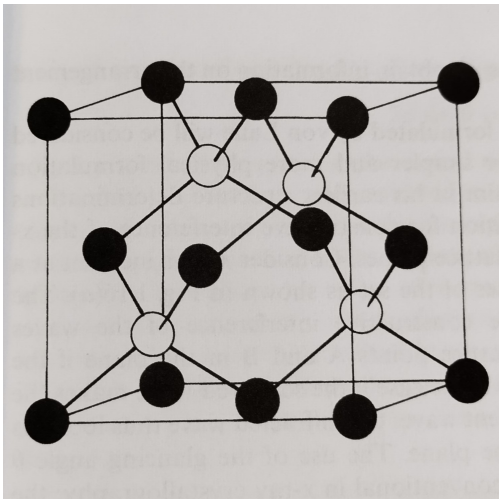

(b) The diamond or ZnS structure. In ZnS the two different coloured circles represent different atoms while in the diamond structure they represent the same atom.[1]

Figure 1: The NaCl and diamond/ZnS structures.

intense than the Kβ line as it is more likely for an electron to fill the K shell from the L shell than from the M shell.[2],[6]

The wavelengths of the characteristic peaks for Mo are: K$\alpha = 71.1$ pm and K$\beta = 63.2$ pm.[2] However it was requested in the lab script to take K$\beta = 63.1$ pm so for the purposes of this experiment it will be taken as such. The spectrum of Mo at 35 kV is shown in figure 2.

As x-ray wavelengths tend to be on the same order as the interatomic spacing in crystals crystals can act as diffraction gratings for x-rays, and so measuring the separation of maxima in the diffraction allows the measurement of the interatomic separation and lattice constant in crystals.[1],[2],[7]

Incident x-rays scatter off of the different lattice planes in the crystal and are reflected. As the lattice planes are physically separated x-rays scattered from one plane will travel a different distance than the x-rays scattered from another plane. Constructive interference occurs when this path difference is equal to a integer number of wavelengths if the x-rays. This is given by Bragg's Law,

$$n\lambda = 2d\sin\beta \tag{1}$$

where n is the order of diffraction and is an integer, λ is the wavelength of the scattered x-rays, d is the spacing of the planes and β is the angle between the incident x-rays and the lattice plane.[1],[2] This is shown in figure 3.

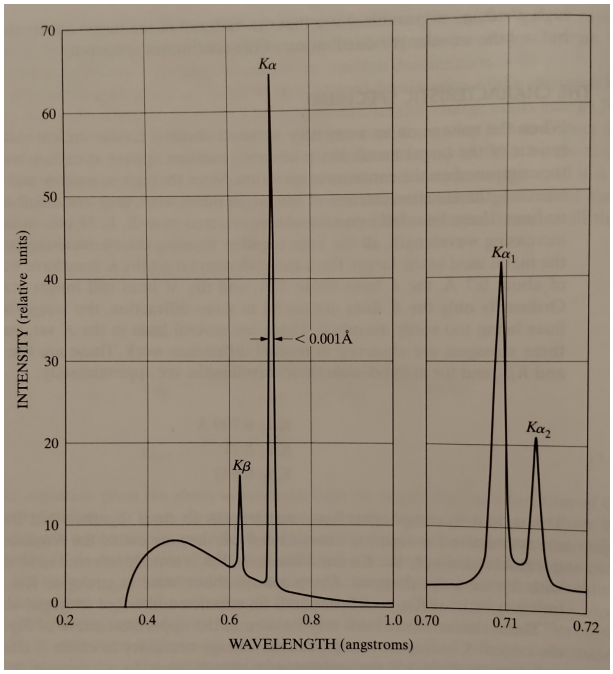

Figure 2: The x-ray spectrum of Mo at 35 kV is shown in the graph on the left, the Kα and Kβ lines are clearly visible. The graph on the right shows the resolved Kα doublet. Note: the line widths are not to scale.[2]

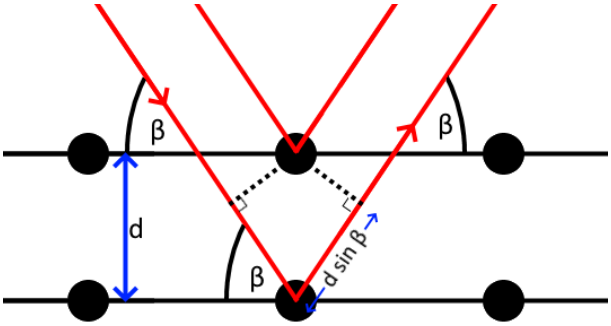

Figure 3: The x-rays are incident at an angle β on the lattice planes separated by a distance d, meaning the path difference between x-rays scattered from adjacent planes is $2d\sin\beta$. For constructive interference to occur between scattered x-rays the path difference must be an integer number of wavelengths, as in equation 1.

The intensity of a scattered wave depends on the type of atom off of which it was scattered and the structure of the crystal which is being studied. Each element has an atomic scattering factor f which depends on the scattering angle and represents the strength of the interaction.[1] In this experiment the scattering angle is the same for each atom at each observed angle and as such that dependency can be ignored.

For cubic crystals this amplitudes produced are

$$A_s = F\begin{cases} 4(f_{Na}+f_{Cl}) & \text{if h, k, l all even} \\ 4(f_{Na}-f_{Cl}) & \text{if h, k, l all odd} \\ 0 & \text{if h, k, l mixed} \end{cases} \tag{2}$$

The ZnS structure has amplitudes of

$$A_s^2 = F^2\begin{cases} (f_{Zn}+f_S)^2 & \text{if } h+k+l=4n \\ (f_{Zn}-f_S)^2 & \text{if } h+k+l=2(2n+1) \\ (f_{Zn}^2+f_S^2) & \text{if h, k, l all odd} \\ (f_{Zn}^2+f_S^2) & \text{if } h+k+l=2(2n+1) \end{cases} \tag{3}$$

The amplitudes of the peaks in a diamond structure are similar to those of the ZnS structure. The amplitude of the scattering is therefore given by

$$A_s^2 = F^2\begin{cases} 4f_C^2 & \text{if } h+k+l=4n \\ 0 & \text{if } h+k+l=2(2n+1) \\ 2f_C^2 & \text{if h, k, l all odd} \\ 2f_C^2 & \text{if } h+k+l=2n+1 \end{cases} \tag{4}$$

In each case F is a constant of proportionality and the specific atomic scattering factors f_{Na}, f_{Cl}, f_{Zn}, f_S and f_C can be replaced by the atomic scattering factor of the appropriate element in that position in the lattice. See Appendix B for the derivations of each of these equations.

For cubic crystals the spacing of the planes, d, can be expressed as

$$d = \frac{a}{\sqrt{h^2+k^2+l^2}} \tag{5}$$

where a is the lattice constant and h,k,l are the indices of the plane. See Appendix C for the derivation of this. From this, equation 1 can be rewritten to give an expression for a,

$$a = \frac{n\lambda\sqrt{h^2+k^2+l^2}}{2\sin\beta} \tag{6}$$

Of course an x-ray source with a continuous spectrum will have diffraction peaks at almost all angles. However, the peaks corresponding to wavelengths of higher intensity will have higher intensity, so for example, with an Mo cathode the peaks corresponding to wavelengths of 71.1 pm and 63.2 pm will be more intense which is very useful in studying the diffraction patterns.[2]

The aim of this experiment is to find the lattice constants for NaCl, LiF, GaP and Si through the x-ray diffraction of NaCl(100), LiF(100), GaP(111), Si(100) and Si(111) crystals.

2 Experimental Details

2.1 General Procedure

The crystal of interest was wiped with the Uvex tissue and placed in the x-ray diffractometer on the support and was clamped firmly against the bar.

The settings on the x-ray diffractometer were set to: U = 35 kV, I = 1 mA, Δt = 1 s, $\Delta\beta = 0.1°$ and the lower and upper limits of β were set to 3.0° and 35.0° respectively. Where U is the tube voltage, I is the current in the tube, Δt is the time spent measuring at each angle, β is the angle of incidence between the sample holder and both the emitter and the detector and $\Delta\beta$ is the amount the angle is changed each step. The "COUPLED" mode was selected. This causes the detector to be rotated through an angle of 2β while the sample holder is only rotated through an angle of β. See figure 4

The scan was started and the spectrum of rate (R) in s^{-1} against angle β was plotted and saved. While, in principle each orientation of the crystal

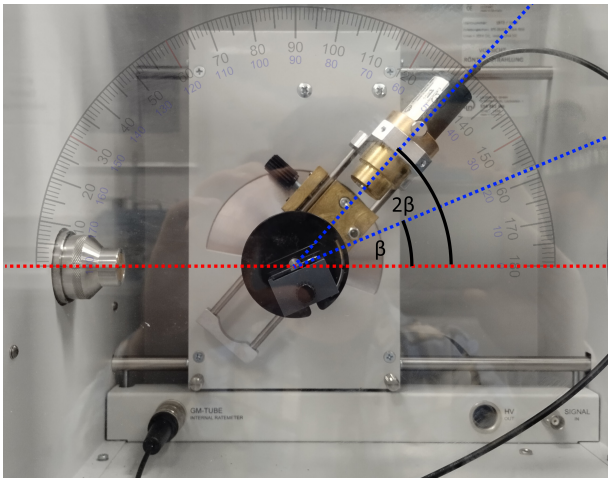

Figure 4: The angle between the incident and scattered rays and the sample in this apparatus is β, while the angle between the detector and the emitted rays is 2β.

should give the same diffraction spectrum the reality is that the crystals are imperfect (for instance the GaP(111) crystal has a crack running through it) and so some orientations are better than others and give clearer spectra. As such, a quick scan with Δt equal to 1 second was carried out for all orientations of the crystal - this is eight orientations for the NaCl(100) crystal and four for the others as they are mounted on glass while NaCl is a solid crystal. Following this the orientation with the highest intensity peaks was chosen to carry out a longer, higher resolution scan with Δt set to 5 seconds with.

In order to differentiate the peaks in the spectrum from the Kα and Kβ emission lines of Mo (whose wavelengths are 71.1 pm and 63.1 pm respectively) a Zr foil filter was placed over the emitter to remove the Kβ radiation, and the diffraction pattern was recorded again. Through comparing this to the unfiltered spectrum the identities of the peaks can be accurately identified, allowing the lattice constant of the crystals to be calculated.

This procedure was carried out for five crystals, NaCl(100), LiF(100), GaP(111), Si(100) and Si(111).

2.2 Repeated Scans of NaCl(100)

When testing the NaCl(100) to find the optimum orientation one orientation was determined to generate the highest intensity peaks. However due to the uniformity of the NaCl crystal this orientation was unfortunately lost. In order to once again find the orientation with the highest intensity peaks the crystal was scanned again at every orientation for angles between $\beta = 3.0°$ and $\beta = 10.0°$ and at a low time resolution of Δt = 1 s. This would reveal the first two peaks in the spectrum and find the orientation with the highest intensity peaks.

Following this high time resolution scans of NaCl(100) in the determined orientation were found for the full range of angles between $\beta = 3.0°$ and $\beta = 35.0°$ as normal.

2.3 Limited Angle Higher Resolution Scans of GaP(111)

The initial high resolution scans of GaP(111) were determined to be very noisy and it was difficult to identify some of the peaks in the data. As such, it was decided to scan the crystal again with the same time resolution and see if the data was any less noisy. Unfortunately it was found to be equally noisy if not more so than the initial scan.

It was then decided to scan the crystal over limited angle ranges which included angles at which peaks were suspected to be present. This was done at a higher time resolution of Δt = 10 s in an effort to reduce the noise and was repeated for the Zr filter placed on the emitter also. The angle ranges chosen were $\beta = [10°, 14°]$, $\beta = [16°, 20°]$ and $\beta = [21°, 27°]$. This produced a less noisy spectrum with more obvious peaks.

3 Results and analysis

3.1 NaCl(100)

The diffraction pattern for NaCl(100) was obtained for each of the eight orientations of the crystal. These diffraction patterns are all shown in figure 5. It can be seen that orientation 7 has the highest intensity peaks and as such that orientation was chosen for the high resolution scan.

As mentioned before however, this orientation was lost, and as such a quick scan between $\beta = 3°$ and $\beta = 10°$ with a Δt of 0.3 s was done to quickly find the orientation with the highest intensity peaks. The results of these scans are shown in figure 6.

Orientation 5 was chosen from these scans as it had high intensity peaks and its peaks were situated closer to the middle of the obtained peaks than those of orientation 8. The high resolution diffraction patterns obtained from this with and without the Zr filter are shown in figure 7.

Using python and the scipy package the peaks, which were found by visual inspection of the diffraction pattern were fitted to Gaussian curves and the

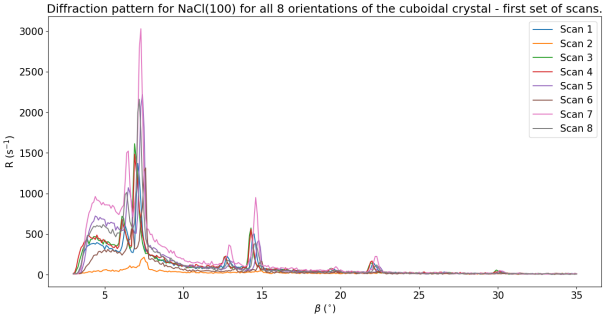

Figure 5: The x-ray diffraction pattern of NaCl for all eight orientations of the crystal between the angles $\beta = 3^\circ$ and $\beta = 35^\circ$.

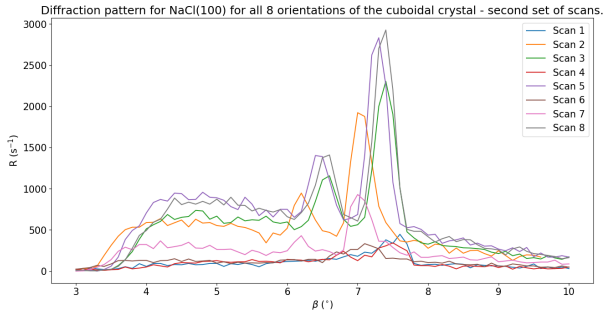

Figure 6: The x-ray diffraction pattern of NaCl(100) for all eight orientations of the crystal between the angles $\beta = 3^\circ$ and $\beta = 10^\circ$.

angle at which they occurred was found (the code is linked in Appendix A). If the peaks occurred in both spectra they were due to the Kα line, while if they occurred in only the unfiltered scan they were due to the Kβ line. The angles of these peaks are shown in table 1.

As shown in equation 2 a diffraction peak will only be visible when h,k,l are all even or all odd. As this crystal has Miller indices (100) peaks will only be visible when h is even (and therefore n is even). The first pair of peaks correspond to n=2, the second pair to n=4, and so on. The lattice constant a_{NaCl} is given by equation 6 , where h=1 and k=l=0. As shown in Appendix D.1 the error in these calculations is given by equation 43. The calculated values for a_{NaCl} from each peak are shown in table 2.

Taking the mean of these values for a_{NaCl}, using equations 45 and 46, the mean calculated value for a_{NaCl} was 5.7 ± 0.4 Å.

All of these values and the mean are consistent with a value of 5.628 Å.[9] However, due to the propagated error a very precise value cannot be obtained, because of the small angles which correspond to the

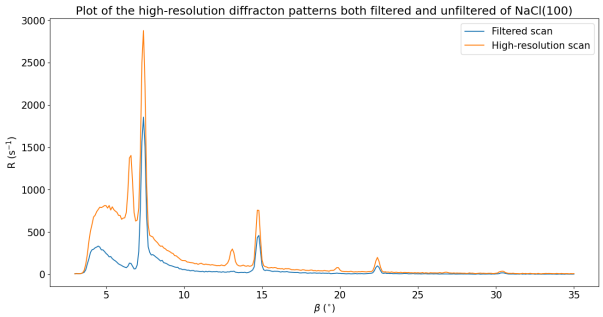

Figure 7: The high-resolution x-ray diffraction pattern of NaCl(100) between the angles $\beta = 3^\circ$ and $\beta = 35^\circ$ obtained both with and without the Zr filter. Peaks due to the Kα line of Mo are visible in both diffraction patterns, while the peaks due to Kβ are only visible in the unfiltered pattern.

Table 1: The angle at which the peaks occur in the diffraction pattern for NaCl(100) as well as which wavelength they are due to.

Peak	angle (°), ±0.05°	Source of peak
1	6.6	Kβ
2	7.4	Kα
3	13.1	Kβ
4	14.7	Kα
5	19.8	Kβ
6	22.4	Kα
7	26.8	Kβ
8	30.4	Kα

more intense peaks which have high relative errors. The precision of the measurement could be improved with a higher angle resolution in the measurements.

3.2 LiF(100)

The diffraction pattern for LiF(100) was obtained for each of the four orientations of the crystal, as well as one of the underside (taken to ensure that the initial four were taken on the correct side of the plate. These diffraction patterns are all shown in figure 8.

Orientation 1 was chosen as the orientation to be used for the high resolution scan, as despite having lower peaks than orientation 2 for the first two peaks it still had significant peaks at these angles, and it had higher peaks than orientation 2 for all other peaks. The high resolution diffraction patterns obtained from this with and without the Zr filter are shown in figure 9.

Similarly to the NaCl(100) peaks, the peaks in the

Table 2: The calculated values for a_{NaCl} for each peak as well as the wavelength which corresponds to each peak.

n	Peak	β (°), ±0.05°	λ (Å)	a_{NaCl} (Å)
2	1	6.6	0.631	5 ± 2
	2	7.4	0.711	6 ± 2
4	3	13.1	0.631	6 ± 1
	4	14.7	0.711	6 ± 1
6	5	19.8	0.631	5.6 ± 0.8
	6	22.4	0.711	5.6 ± 0.7
8	7	26.8	0.631	5.6 ± 0.6
	8	30.4	0.711	5.6 ± 0.5

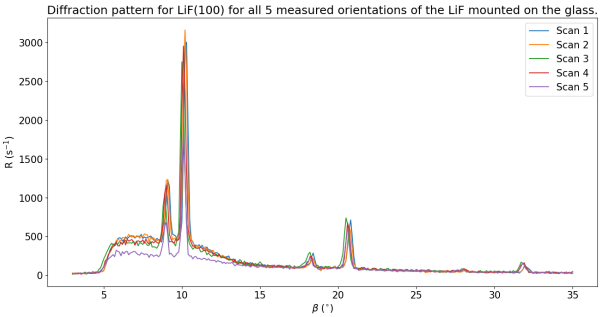

Figure 8: The x-ray diffraction pattern of LiF(100) for all five orientations of the crystal between the angles $\beta = 3°$ and $\beta = 35°$.

diffraction pattern of LiF(100) were found through visual inspection and were then fitted using python and the scipy package to Gaussian curves to find the angle at which their peaks occurred (the code is linked in Appendix A). If the peaks occurred in both spectra they were due to the Kα line, while if they occurred in only the unfiltered scan they were due to the Kβ line. The angles of these peaks are shown in table 3.

Table 3: The angle at which the peaks occur in the diffraction pattern for LiF(100) as well as which wavelength they are due to.

Peak	angle (°), ±0.05°	Source of peak
1	8.9	Kβ
2	10.1	Kα
3	18.2	Kβ
4	20.6	Kα
5	27.9	Kβ
6	31.8	Kα

Similarly to NaCl(100), the diffraction pattern will show a peak only when n is even. And the first pair of peaks corresponds to n=2, the second pair to n=4, etc. The lattice constant a_{LiF} is given by equation 6,

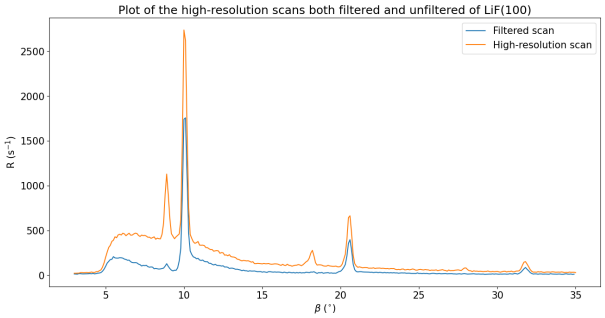

Figure 9: The high-resolution x-ray diffraction pattern of Lif(100) between the angles $\beta = 3°$ and $\beta = 35°$ obtained both with and without the Zr filter. Peaks due to the Kα line of Mo are visible in both diffraction patterns, while the peaks due to Kβ are only visible in the unfiltered pattern.

where h=1 and k=l=0. As shown in Appendix D.1 the error in these calculations is given by equation 43. The calculated values for a_{LiF} from each peak are shown in table 4.

Table 4: The calculated values for a_{LiF} for each peak as well as the wavelength which corresponds to each peak.

n	Peak	β (°), ±0.05°	λ (Å)	a_{LiF} (Å)
2	1	8.9	0.631	4 ± 1
	2	10.1	0.711	4 ± 1
4	3	18.2	0.631	4.0 ± 0.6
	4	20.6	0.711	4.0 ± 0.5
6	5	27.9	0.631	4.0 ± 0.4
	6	31.8	0.711	4.0 ± 0.3

Taking the mean of these values for a_{LiF}, using equations 45 and 46 as above, the mean calculated value for a_{LiF} was 4.0 ± 0.3 Å.

All of these values and the mean are consistent with a value of 4.017 Å.[9] However, due to the propagated error a very precise value cannot be obtained, because of the small angles which correspond to the more intense peaks which have high relative errors. The precision of the measurement could be improved with a higher angle resolution in the measurements.

3.3 GaP(111)

The diffraction pattern for GaP(111) was obtained for each of the four orientations of the crystal. These diffraction patterns are all shown in figure 10.

Orientation 1 was chosen as the orientation to be used for the high resolution scan, . The high resolution diffraction patterns obtained from this with and without the Zr filter are shown in figure 11.

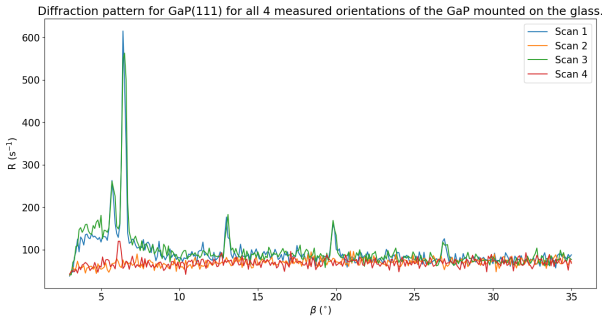

Figure 10: The x-ray diffraction pattern of GaP(111) for all four orientations of the crystal between the angles $\beta = 3°$ and $\beta = 35°$.

Figure 11: The high-resolution x-ray diffraction pattern of GaP(111) between the angles $\beta = 3°$ and $\beta = 35°$ obtained both with and without the Zr filter. Peaks due to the Kα line of Mo are visible in both diffraction patterns, while the peaks due to Kβ are only visible in the unfiltered pattern.

As stated previously, the peaks of the unfiltered scan are indistinct due to a high level of noise, and so another diffraction pattern with the same settings was obtained and is shown in figure 12.

However, the noise was equally as high in this pattern as in the previous one, so scans of limited angles where peaks were suspected were carried out with Δt = 10 s both with and without the Zr filter. The results of this are shown in figure 13

It can clearly be seen in this image that there are peaks due to the Mo Kβ line visible at approximately 11.6°, 17.6° and 23.7°. Similarly to LiF(100) and NaCl(100) the positions of the peaks were found using python and scipy by fitting them with Gaussian curves (the code is linked in Appendix A). Again, if peaks were visible in both spectra they were due to the Kα line, while if they occurred in only the unfiltered scan they were due to the Kβ line. The angles of these peaks are shown in table 5.

Unlike that of NaCl(100) or LiF(100), as GaP has

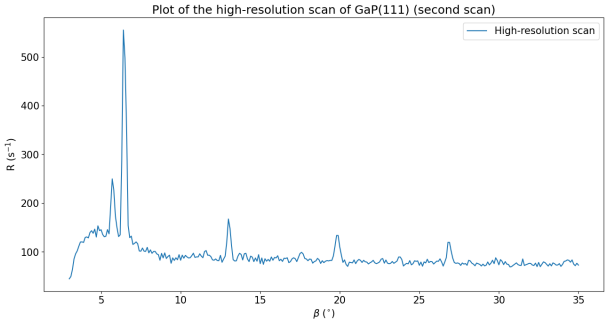

Figure 12: The second high-resolution x-ray diffraction pattern obtained GaP(111) between the angles $\beta = 3°$ and $\beta = 35°$.

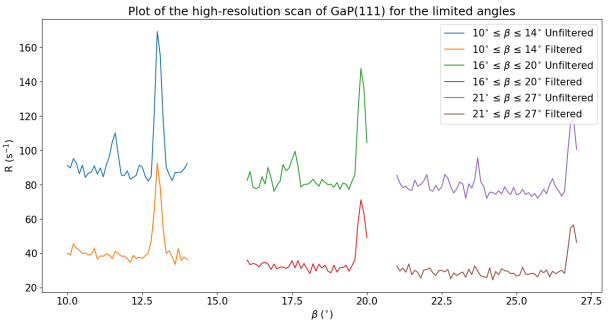

Figure 13: The high-resolution x-ray diffraction pattern obtained GaP(111) between the for the limited angle ranges $\beta = [10°, 14°]$, $\beta = [16°, 20°]$ and $\beta = [21°, 27°]$.

a zinc blende structure and this crystal has the Miller indices (111), the diffraction pattern shows peaks associated with values where h, k and l are all odd, and when $h + k + l$ is an even number, as stated in equation 3.

The diffraction patterns show four pairs of peaks. If these are taken as n=1, n=2, n=3 and n=4 respectively then the Miller indices in each case are (111), (222), (333) and (444) respectively. Checking each of these values it can be seen clearly that in the case of n=1 and n=3 there is a peak as h, k and l are all odd. In the case of n=2 and n=4 the sum of h, k and l is an even number, and so, again they would produce a peak. Therefore, the peaks are indeed due to diffraction where n=1, n=2, n=3 and n=4 respectively.

The lattice constant a_{GaP} is given by equation 6, where h=k=l=1. As shown in Appendix D.1 the error in these calculations is given by equation 43. The calculated values for a_{GaP} from each peak are shown in table 6.

Taking the mean of these values for a_{GaP}, using equations 45 and 46 as above, the mean calculated

Table 5: The angle at which the peaks occur in the diffraction pattern for GaP(111) as well as which wavelength they are due to.

Peak	angle (°), ±0.05°	Source of peak
1	5.7	Kβ
2	6.5	Kα
3	11.6	Kβ
4	13.0	Kα
5	17.5	Kβ
6	19.8	Kα
7	23.7	Kβ
8	26.9	Kα

Table 6: The calculated values for a_{GaP} for each peak as well as the wavelength which corresponds to each peak.

n	Peak	β (°), ±0.05°	λ (Å)	a_{GaP} (Å)
1	1	5.7	0.631	6 ± 3
	2	6.5	0.711	5 ± 2
2	3	11.6	0.631	5.4 ± 1
	4	13.0	0.711	5.5 ± 1
3	5	17.5	0.631	5.5 ± 0.9
	6	19.8	0.711	5.5 ± 0.8
4	7	23.7	0.631	5.4 ± 0.6
	8	26.9	0.711	5.4 ± 0.5

value for a_{GaP} was 5.5 ± 0.5 Å.

All of these values and the mean are consistent with a value of 5.4905 Å.[5] However, due to the propagated error a very precise value cannot be obtained, because of the small angles which correspond to the more intense peaks which have high relative errors. The precision of the measurement could be improved with a higher angle resolution in the measurements.

3.4 Si(100)

The diffraction pattern for Si(100) was obtained for each of the four orientations of the crystal. These diffraction patterns are all shown in figure 14.

Orientation 4 was chosen as the orientation to be used for the high resolution scan, . The high resolution diffraction patterns obtained from this with and without the Zr filter are shown in figure 15.

Similarly to the previous crystals, the peaks in the diffraction pattern of Si(100) were found through visual inspection and were then fitted using python and the scipy package to Gaussian curves to find the angle at which their peaks occurred (the code is linked in Appendix A). If the peaks occurred in both spectra they were due to the Kα line, while if they occurred in only the unfiltered scan they were due to the Kβ line. The angles of these peaks are shown in table 7.

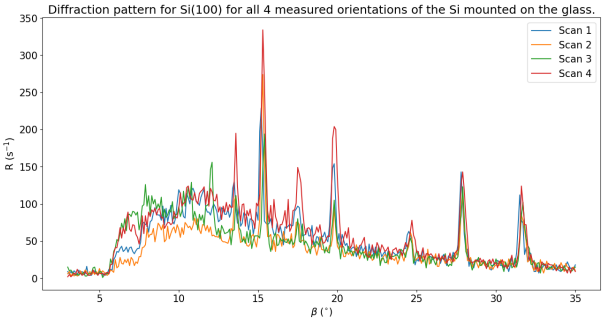

Figure 14: The x-ray diffraction pattern of Si(100) for all four orientations of the crystal between the angles $\beta = 3°$ and $\beta = 35°$.

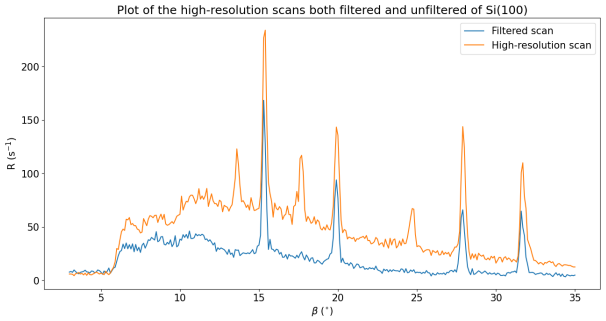

Figure 15: The high-resolution x-ray diffraction pattern of Si(100) between the angles $\beta = 3°$ and $\beta = 35°$ obtained both with and without the Zr filter. Peaks due to the Kα line of Mo are visible in both diffraction patterns, while the peaks due to Kβ are only visible in the unfiltered pattern.

Interestingly, the peaks usually occur in pairs, with a peak due to the Mo Kβ line directly preceding a peak due to the Kα line. This trend is apparently violated for the seventh peak in this diffraction pattern as it is due to the Kα line and appears to have no corresponding Kβ peak. However, if it is assumed that peak six is a combination of both the Kα and Kβ lines, due to its unusual height and its close proximity to the seventh peak, it is found that it gives a very accurate value for the lattice constant, a_{Si}, and so it is likely that this is the case.

Taking the observed pairs of peaks in the diffraction pattern corresponding to n=1, n=3, n=4 and n=5 (with the peak at 27.9° being shared between n=4 and n=5) the lattice constant, a_{Si}, is found using equation 6, where h=1 and k=l=0. As shown in Appendix D.1 the error in these calculations is given by equation 43. The calculated values for a_{Si} from each peak are shown in table 8.

Table 7: The angle at which the peaks occur in the diffraction pattern for Si(100) as well as which wavelength they are due to.

Peak	angle (°), ±0.05°	Source of peak
1	13.6	Kβ
2	15.4	Kα
3	17.7	Kβ
4	19.9	Kα
5	24.7	Kβ
6	27.9	Kα
7	31.7	Kα

Table 8: The calculated values for a_{GaP} for each peak as well as the wavelength which corresponds to each peak.

n	Peak	β (°), ±0.05°	λ (Å)	a_{GaP} (Å)
1	1	13.6	0.631	1.3 ± 0.3
	2	15.4	0.711	1.3 ± 0.2
3	3	17.7	0.631	3.1 ± 0.5
	4	19.9	0.711	3.1 ± 0.4
4	5	24.7	0.631	3.0 ± 0.3
	6	27.9	0.711	3.0 ± 0.3
5	7	27.9	0.631	3.4 ± 0.3
	8	31.7	0.711	3.4 ± 0.3

Taking the mean of these values for a_{Si}, using equations 45 and 46 as above, the mean calculated value for a_{Si} was 2.7 ± 0.1 Å.

None of these values are close to a value of 5.43072 Å.[4] However, the peaks do not appear until 13.6°, so it is not unreasonable to suspect that there may be other peaks which did not appear in the diffraction patterns in figure 15. Indeed, if "Scan 3" from figure 14 is studied there appear to be at least three other peaks occurring at angles less than 13.6°. "Scan 3" is shown separately in figure 16

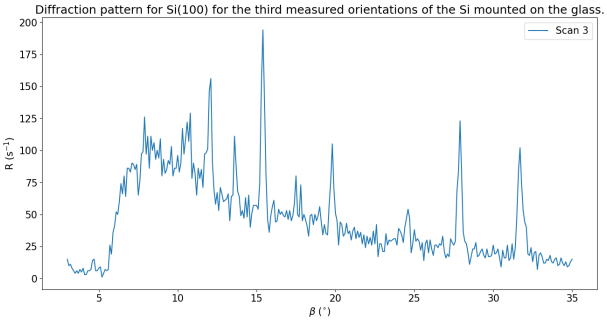

Figure 16: The x-ray diffraction pattern of Si(100) for "Scan 3" as shown in figure 14.

Unfortunately there was no high-resolution diffraction pattern taken for this orientation, as this was not noticed until writing the report as no other orientations produced a diffraction pattern of this shape so it was determined that this was likely noise or a defect. As such the graph in figure 15 must be made do with. If it is assumed that there are peaks corresponding to n=1 and n=3 (there are no peaks corresponding to n=2 in accordance with equation 3) which do not appear in figure 15 and that the visible peaks correspond to n=4, n=5, n=7 and n=8 (with the peak at 27.9° being shared between n=7 and n=8) a_{Si} can be found again using equation 6. The newly calculated values for a_{Si} corresponding to each peak are shown in table 9.

Table 9: The calculated values for a_{GaP} for each peak as well as the wavelength which corresponds to each peak.

n	Peak	β (°), ±0.05°	λ (Å)	a_{GaP} (Å)
4	1	13.6	0.631	5 ± 1
	2	15.4	0.711	5 ± 1
5	3	17.7	0.631	5.2 ± 0.8
	4	19.9	0.711	5.2 ± 0.7
7	5	24.7	0.631	5.3 ± 0.6
	6	27.9	0.711	5.3 ± 0.5
8	7	27.9	0.631	5.4 ± 0.5
	8	31.7	0.711	5.4 ± 0.4

Taking the mean of these values for a_{Si}, using equations 45 and 46 as above, the mean calculated value for a_{Si} was 5.2 ± 0.3 Å.

It is odd that the two different orientations produced such significantly different diffraction patterns. This is likely due to defects in the crystal.

All of these values and the mean are consistent with a value of 5.43072 Å.[4] However, due to the propagated error a very precise value cannot be obtained, because of the small angles which correspond to the more intense peaks which have high relative errors. The precision of the measurement could be improved with a higher angle resolution in the measurements.

A more accurate value for a_{Si} could be obtained from this by taking a higher time resolution diffraction pattern using orientation 3 and calculating a_{Si} using the angles obtained there.

3.5 Si(111)

The diffraction pattern for Si(111) was obtained for each of the four orientations of the crystal. These diffraction patterns are all shown in figure 17.

Orientation 4 was chosen as the orientation to be used for the high resolution scan, . The high resolution diffraction patterns obtained from this with and

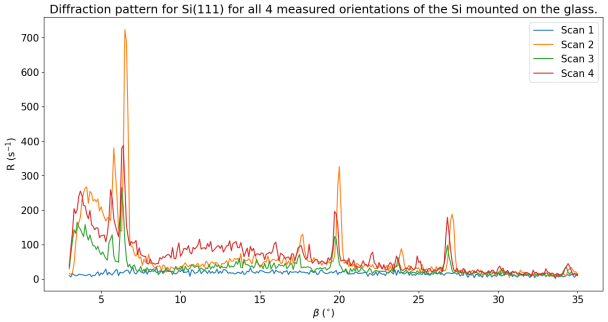

Figure 17: The x-ray diffraction pattern of Si(111) for all four orientations of the crystal between the angles $\beta = 3°$ and $\beta = 35°$.

without the Zr filter are shown in figure 18.

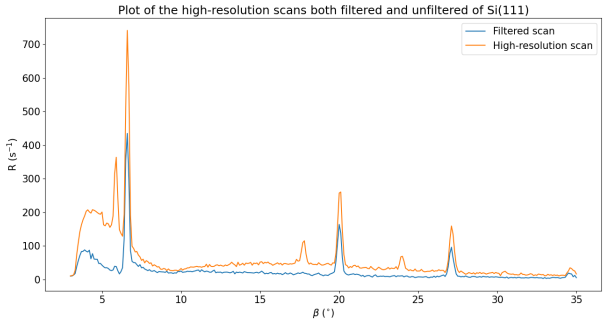

Figure 18: The high-resolution x-ray diffraction pattern of Si(111) between the angles $\beta = 3°$ and $\beta = 35°$ obtained both with and without the Zr filter. Peaks due to the Kα line of Mo are visible in both diffraction patterns, while the peaks due to Kβ are only visible in the unfiltered pattern.

Similarly to the previous crystals, the peaks in the diffraction pattern of Si(111) were found through visual inspection and were then fitted using python and the scipy package to Gaussian curves to find the angle at which their peaks occurred (the code is linked in Appendix A). If the peaks occurred in both spectra they were due to the Kα line, while if they occurred in only the unfiltered scan they were due to the Kβ line. The angles of these peaks are shown in table 10.

Again, despite the peaks usually occurring in pairs the seventh peak occurs on its own, with no corresponding Kβ peak. This may be because the peaks at this angle have become much less intense, and so it may be there and just be indistinguishable from the noise in the data.

The conditions for a peak to be observed according to equation 4 are fulfilled for n=1, n=3, n=4 and n=5.

Table 10: The angle at which the peaks occur in the diffraction pattern for Si(111) as well as which wavelength they are due to.

Peak	angle (°), ±0.05°	Source of peak
1	5.9	Kβ
2	6.6	Kα
3	17.7	Kβ
4	20.0	Kα
5	24.0	Kβ
6	27.1	Kα
7	34.7	Kα

The lattice constant a_{GaP} is given by equation 6, where h=k=l=1. As shown in Appendix D.1 the error in these calculations is given by equation 43. The calculated values for a_{Si} from each peak are shown in table 11.

Table 11: The calculated values for a_{Si} for each peak as well as the wavelength which corresponds to each peak.

n	Peak	β (°), ±0.05°	λ (Å)	a_{GaP} (Å)
1	1	5.9	0.631	5 ± 3
	2	6.6	0.711	5 ± 2
3	3	17.7	0.631	5.4 ± 0.8
	4	20.0	0.711	5.4 ± 0.7
4	5	24.0	0.631	5.4 ± 0.6
	6	27.1	0.711	5.4 ± 0.5
5	7	34.7	0.711	5.4 ± 0.4

Taking the mean of these values for a_{Si}, using equations 45 and 46 as above, the mean calculated value for a_{Si} was 5.3 ± 0.6 Å.

All of these values and the mean are consistent with a value of 5.43072 Å.[4] However, due to the propagated error a very precise value cannot be obtained, because of the small angles which correspond to the more intense peaks which have high relative errors. The precision of the measurement could be improved with a higher angle resolution in the measurements.

4 Conclusions

The lattice constants for NaCl, Lif, GaP and crystalline Si were measured using x-ray diffraction. The mean values for each measurement are shown below in table 12

If only the second and third of the three values of a_{Si} are accepted then the average value for a_{Si} is 5.3 ± 0.3.

Table 12: The lattice constants of NaCl, Lif, GaP and crystalline Si.

Crystal	a (Å)
NaCl	5.7 ± 0.4
LiF	4.0 ± 0.3
GaP	5.5 ± 0.5
Si(100) (starting from n=1)	2.7 ± 0.1
Si(100) (starting from n=4)	5.2 ± 0.3
Si(111)	5.3 ± 0.6

Apart from the value for a_{Si} from Si(100) starting from n=1 all of these values are consistent with the literature values for the lattice constants, with $a_{NaCl} = 5.628$ Å, $a_{LiF} = 4.017$ Å, $a_{GaP} = 5.4905$ Å and $a_{Si} = 5.43072$ Å.[4],[5],[9]

Subsequent scans with higher angle resolution will allow for more precise measurements of a while a higher time resolution could allow for further improved accuracy.

Another Si(100) sample could also be used if possible, as it appears that there are defects in the current crystal which lead certain peaks to be visible only at certain orientations. This may be due to the experimental practice and procedure, however as this issue was noticed for no other crystals, or even any of the higher order peaks in the Si(100) diffraction pattern, it is likely not an issue with the procedure or the apparatus themselves.

The fitting of the peaks to Gaussian curves worked very well, however it is possible that there are better functions which could be used instead of/as well as Gaussian curves. This could be investigated further.

A Code and original data

The code and original data for this experiment can be found here. (https://github.com/ismisebrendan/Xray_Diffraction)

B Derivation of Scattering Amplitudes

This is generally true for the three structures in this experiment, only the geometry is different and so the general derivation will be carried out once here and more specifically in the separate sections for each structure.

For an atom at position $\vec{r}$ in a crystal if a plane wave of initial amplitude A_0 is incident on it the amplitude of the scattered wave (A_s) at a detector at position $\vec{R}$ is given by

$$A_s = A_0 e^{i(\vec{k}\cdot\vec{r}-\omega t)} \times f \times \frac{e^{ik|\vec{R}-\vec{R}|}}{|\vec{R}-\vec{R}|} \tag{7}$$

where $A_0 e^{i(\vec{k}\cdot\vec{r}-\omega t}$ is the equation of the initial wave, f is the aforementioned atomic scattering factor and $\frac{e^{ik|\vec{R}-\vec{R}|}}{|\vec{R}-\vec{R}|}$ accounts for the decrease in amplitude and phase change when viewed at the detector.[1]

As the amplitude decrease due to each atom is effectively the same when viewed at a large distance the $\frac{1}{|\vec{R}-\vec{R}|}$ factor can be replaced by $\frac{1}{R}$ where R is the distance between the crystal and the detector. The wave incident at the detector has a wavevector $\vec{k'}$ of approximately the same amplitude as $\vec{k}$, the initial wavevector, and it is approximately parallel to $\vec{R}$ and $\vec{R}-\vec{r}$. So the approximation

$$\begin{aligned} k|\vec{R}-\vec{r}| &\approx \vec{k'}\cdot(\vec{R}-\vec{r}) = \vec{k'}\cdot\vec{R} - \vec{k'}\cdot\vec{r} \\ &\approx kR - \vec{k'}\cdot\vec{r} \end{aligned} \tag{8}$$

can be made.[1]

Allowing equation7 to be rewritten as

$$A_s = A_0 \frac{e^{i(kR-\omega t)}}{R} f\, e^{-i(\vec{K})\cdot\vec{r}} \tag{9}$$

where $\vec{K} = \vec{k'} - \vec{k}$, the scattering vector. The $A_0\frac{e^{i(kR-\omega t)}}{R}$ factor is identical for all atoms in the crystal, meaning the final amplitude of the scattered wave due to n atoms in the crystal (A_s) is proportional to the sum of the atomic scattering factors and the final factor which is due to the phase differences caused by scattering from the m different atoms.[1] This can be expressed as

$$A_s \propto \sum_m f_m\, e^{-i\vec{K}\cdot\vec{r_m}} \tag{10}$$

The vector $\vec{r_m}$ depends on both the position of the lattice point $\vec{r_l}$ and the position of the atom within the basis $\vec{r_p}$., so $\vec{r_m} = \vec{r_l} + \vec{r_p}$.[1] And so equation 10 can be rewritten as

$$A_s \propto \sum_l e^{-i\vec{K}\cdot\vec{r_l}} \sum_p f_p e^{-i\vec{K}\cdot\vec{r_p}} \tag{11}$$

Taking the second summation term in equation 11,

$$\sum_p f_p e^{-i\vec{K}\cdot\vec{r_p}} \tag{12}$$

the amplitude due to the scattering from a single unit cell can be found. The position of an atom in a cubic unit cell can be expressed as

$$r_p = u\vec{a} + v\vec{b} + w\vec{c} \tag{13}$$

where u, v, w are positive real numbers less than or equal to 1 and $\vec{a}, \vec{b}, \vec{c}$ are the basis vectors for the lattice.

When a large peak is observed due to diffraction scattering the scattering vector, $\vec{K}$ can be expressed as

$$\vec{K} = h\vec{a}^* + k\vec{b}^* + l\vec{c}^* \tag{14}$$

where $\vec{a}^*, \vec{b}^*, \vec{c}^*$ are given by

$$\vec{a}^* = \frac{2\pi(\vec{b} \times \vec{c})}{\vec{a} \cdot (\vec{b} \times \vec{c})} \tag{15}$$

$$\vec{b}^* = \frac{2\pi(\vec{c} \times \vec{a})}{\vec{a} \cdot (\vec{b} \times \vec{c})} \tag{16}$$

$$\vec{c}^* = \frac{2\pi(\vec{a} \times \vec{b})}{\vec{a} \cdot (\vec{b} \times \vec{c})} \tag{17}$$

and are the primitive reciprocal lattice vectors.[1]

It can be seen clearly and should be noted that $\vec{a}^* \cdot \vec{a} = 2\pi$, $\vec{b}^* \cdot \vec{a} = 0$ and $\vec{c}^* \cdot \vec{a} = 0$. This is similar for the vectors $\vec{b}$ and $\vec{c}$, $\vec{b}^* \cdot \vec{b} = 2\pi$ and $\vec{c}^* \cdot \vec{c} = 2\pi$ while everything else is equal to 0.[8]

This allows equation 12 to be rewritten as

$$\sum_p f_p e^{-i\vec{K}\cdot\vec{r_p}} = \sum_p f_p e^{-i(h\vec{a}^*+k\vec{b}^*+l\vec{c}^*)\cdot(u\vec{a}+v\vec{b}+w\vec{c})} \tag{18}$$

And so

$$A_s = F\sum_p f_p e^{-i(h\vec{a}^*+k\vec{b}^*+l\vec{c}^*)\cdot(u\vec{a}+v\vec{b}+w\vec{c})} \tag{19}$$

Where F is a proportionality constant

B.1 NaCl Structure

Equation 19 can now be evaluated for the ions in the basis of NaCl. As shown in figure 19 there are eight ions in the basis.

The positions of the four Na^+ ions are:

$$\vec{r_1} = 0, \vec{r_2} = 0.5\vec{a}+0.5\vec{b}, \vec{r_3} = 0.5\vec{a}+0.5\vec{c}, \vec{r_4} = 0.5\vec{b}+0.5\vec{c}$$

While the positions of the Cl^- ions are:

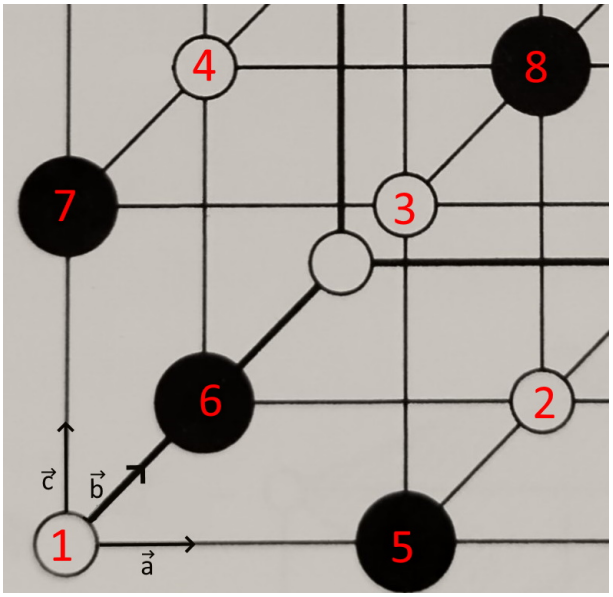

Figure 19: The atoms in the unit cell of NaCl labelled, with the Na^+ ions labelled 1-4 and the Cl^- ions labelled 5-8. Adapted from [2]

$$\vec{r_5} = 0.5\vec{a}, \vec{r_6} = 0.5\vec{b}, \vec{r_7} = 0.5\vec{c}, \vec{r_8} = 0.5\vec{a}+0.5\vec{b}+0.5\vec{c}$$

Rewriting equation 19 as

$$A_s = F\left(f_{Na}\sum_{m=1}^{4} e^{-i\vec{K}\cdot\vec{r_m}} + f_{Cl}\sum_{m=5}^{8} e^{i\vec{K}\cdot\vec{r_m}}\right) \tag{20}$$

We get

$$\frac{A_s}{F} = f_{Na}\left(e^0 + e^{-i\pi(h+k)} + e^{-i\pi(h+l)} + e^{-i\pi(k+l)}\right) + f_{Cl}\left(e^{-i\pi(h)} + e^{-i\pi(k)} + e^{-i\pi(l)} + e^{-i\pi(h+k+l)}\right) \tag{21}$$

We then use the following facts, $e^{-i\pi n} = 1$ for even n and $e^{-i\pi n} = -1$ for odd n where n is an integer.

For $q_1, q_2, q_3 \in \mathbb{Z}$ the following statements are true

- $2q_1 + 2q_2 + q_3 = 2(q_1 + q_2 + q_3)$ - the sum of solely even numbers is even.
- $(2q_1 + 1) + (2q_2 + 1) = 2(q_1 + q_2 + 1)$ - the sum of two odd numbers is even.
- $(2q_1 + 1) + (2q_2 + 1) + (2q_3 + 1) = 2(q_1 + q_2 + q_3 + 1) + 1$ - the sum of three odd numbers is odd.

- $(2q_1+1)+2q_2 = 2(q_1+q_2)+1$ - the sum of an odd number and an even number is odd.

From this it can be seen that for h, k, l all even equation 21 becomes:

$$\begin{aligned} A_s &= F(f_{Na}(1+1+1+1)+f_{Cl}(1+1+1+1) \\ &= 4F(f_{Na}+f_{Cl}) \end{aligned} \tag{22}$$

For h, k, l all odd it becomes:

$$\begin{aligned} A_s &= F(f_{Na}(1+1+1+1)+f_{Cl}(-1-1-1-1) \\ &= 4F(f_{Na}-f_{Cl}) \end{aligned} \tag{23}$$

When h, k, l are mixed two must have the same parity, here it will be taken that h and k are both even and l is odd, however in reality it does not matter which is which. As such equation 21 becomes:

$$\begin{aligned} A_s &= F(f_{Na}(1+1-1-1)+f_{Cl}(1+1-1-1) \\ &= 0 \end{aligned} \tag{24}$$

This is all summarised in equation 25.

$$A_s = F\begin{cases} 4(f_{Na}+f_{Cl}) & \text{if h, k, l all even} \\ 4(f_{Na}-f_{Cl}) & \text{if h, k, l all odd} \\ 0 & \text{if h, k, l mixed} \end{cases} \tag{25}$$

B.2 ZnS Structure

The ZnS or diamond structure has a two atom basis, with the atoms being located at $\vec{r_1} = 0$ and $\vec{r_2} = 0.25\vec{a}+0.25\vec{b}+0.25\vec{c}$ respectively.[1]

Taking Zn as atom 1 and S as atom 2 and evaluating equation 19 we get

$$\begin{aligned} A_s &= F(f_{Zn}e^0 + f_S e^{-i\frac{\pi}{2}(h+k+l)}) \\ &= F(f_{Zn}+f_S e^{-i\frac{\pi}{2}(h+k+l)}) \end{aligned} \tag{26}$$

Using the same relations as in Appendix B.1 it is found that for $h+k+l = 4n$

$$\begin{aligned} A_s &= F(f_{Zn}+f_S e^{-i\frac{\pi}{2}(4n)}) \\ &= F(f_{Zn}+f_S e^{-2in\pi}) \\ &= F(f_{Zn}+f_S) \end{aligned} \tag{27}$$

For $h+k+l+2(n+1)$

$$\begin{aligned} A_s &= F(f_{Zn}+f_S e^{-i\frac{\pi}{2}(2(n+1))}) \\ &= F(f_{Zn}+f_S e^{-i\pi(2n+1)}) \\ &= F(f_{Zn}-f_S) \end{aligned} \tag{28}$$

For h, k, l all odd

$$\begin{aligned} A_s &= F(f_{Zn}+f_S e^{-i\frac{\pi}{2}(h+k+l)}) \\ &= F(f_{Zn}+f_S e^{-i\frac{\pi}{2}(2n+1)}) \\ &= F(f_{Zn}+f_S e^{-i\pi n-\frac{\pi}{2}}) \\ &= F(f_{Zn}+(-1)^n i\, f_S) \end{aligned} \tag{29}$$

And for $h+k+l = 2n+1$ (odd)

$$\begin{aligned} A_s &= F(f_{Zn}+f_S e^{-i\frac{\pi}{2}(2n+1)}) \\ &= F(f_{Zn}+f_S e^{-i\frac{\pi}{2}(2n+1)}) \\ &= F(f_{Zn}+f_S e^{-i\pi n-\frac{\pi}{2}}) \\ &= F(f_{Zn}+(-1)^n i\, f_S) \end{aligned} \tag{30}$$

This gives

$$A_s = F\begin{cases} (f_{Zn}+f_S) & \text{if } h+k+l = 4n \\ (f_{Zn}-f_S) & \text{if } h+k+l = 2(2n+1) \\ (f_{Zn}+(-1)^n i\, f_S) & \text{if h, k, l all odd} \\ (f_{Zn}+(-1)^n i\, f_S) & \text{if } h+k+l = 2n+1 \end{cases} \tag{31}$$

If the amplitude is taken to make the values real

$$A_s^2 = F^2\begin{cases} (f_{Zn}+f_S)^2 & \text{if } h+k+l = 4n \\ (f_{Zn}-f_S)^2 & \text{if } h+k+l = 2(2n+1) \\ (f_{Zn}^2+f_S^2) & \text{if h, k, l all odd} \\ (f_{Zn}^2+f_S^2) & \text{if } h+k+l = 2(2n+1) \end{cases} \tag{32}$$

B.3 Diamond Structure

Taking equation 32 and letting $f_{Zn} = f_S = f_C$ we get

$$A_s^2 = F^2\begin{cases} (2f_C)^2 & \text{if } h+k+l = 4n \\ (f_C-f_C)^2 & \text{if } h+k+l = 2(2n+1) \\ 2f_C^2 & \text{if h, k, l all odd} \\ 2f_C^2 & \text{if } h+k+l = 2(2n+1) \end{cases}$$

$$A_s^2 = F^2 \begin{cases} 4f_C^2 & \text{if } h+k+l = 4n \\ 0 & \text{if } h+k+l = 2(2n+1) \\ 2f_C^2 & \text{if h, k, l all odd} \\ 2f_C^2 & \text{if } h+k+l = 2(2n+1) \end{cases} \quad (33)$$

C Derivation of Equation 5

The lattice planes of a cubic crystal have an x-intercept of $(\frac{na}{h}, 0, 0)$ where n is an integer, and a lattice plane with Miller indices [hkl] is perpendicular to the direction (h,k,l).[2] From the well-known equation of a plane $\vec{n} \cdot (x - x_0, y - y_0, z - z_0) = 0$ where $\vec{n}$ is the normal vector to the plane of the form (α, β, γ) and $P_0 = (x_0, y_0, z_0)$ is a point on the plane this gives a general equation of a plane

$$\alpha x + \beta y + \gamma z - (\alpha x_0 + \beta y_0 + \gamma z_0) = 0 \quad (34)$$

Therefore the general equation of a lattice plane for a cubic crystal is given by

$$(h,k,l) \cdot (x - \frac{na}{h}, y, z) = hx + yk + zl - na = 0 \quad (35)$$

So two adjacent planes with n = 1 and n = 2 have equations

$$hx + yk + zl - a = 0 \quad (36)$$

and

$$hx + yk + zl - 2a = 0 \quad (37)$$

respectively.

The distance (d) between a point $P_1 = (x_1, y_1, z_1)$ and a plane $\alpha x + \beta y + \gamma z - \delta = 0$ which has a point $P_0 = (x_0, y_0, z_0)$ on it is the magnitude of the projection of the vector $\overrightarrow{P_0P_1}$ between the two points onto the unit normal vector of the plane, $\hat{n} = \frac{\vec{n}}{|\vec{n}|}$, which is given by

$$\begin{aligned} d &= \frac{|\overrightarrow{P_0P_1} \cdot \vec{n}|}{|\vec{n}|} \\ &= \frac{|(x_1 - x_0, y_1 - y_0, z_1 - z_0) \cdot (\alpha, \beta, \gamma)|}{\sqrt{\alpha^2 + \beta^2 + \gamma^2}} \\ &= \frac{|\alpha x_1 + \beta y_1 + \gamma z_1 - (\alpha x_0 + \beta y_0 + \gamma z_0)|}{\sqrt{\alpha^2 + \beta^2 + \gamma^2}} \\ &= \frac{|\alpha x_1 + \beta y_1 + \gamma z_1 - \delta|}{\sqrt{\alpha^2 + \beta^2 + \gamma^2}} \end{aligned} \quad (38)$$

Substituting the values for the lattice planes into this, for the point on the n = 1 lattice plane, $P_1 = (\frac{a}{h}, 0, 0)$ and the n = 2 lattice plane $hx+yk+zl-2a = 0$ gives

$$\begin{aligned} d &= \frac{|a - 2a|}{\sqrt{h^2 + k^2 + l^2}} \\ &= \frac{a}{\sqrt{h^2 + k^2 + l^2}} \end{aligned} \quad (39)$$

as required.

D Propagation of Error

D.1 Determination of the Lattice Constant from the Angle of the Peak

From Gauss' error law, for an equation $y = f(x)$, the error in y, Δy is given by

$$\Delta y = \sqrt{\left(\frac{\partial y}{\partial x} \Delta x\right)^2} \quad (40)$$

For equation 6,

$$a = \frac{n\lambda\sqrt{h^2 + k^2 + l^2}}{2 \sin \beta}$$

the only value with uncertainty is β. Therefore the error in a, Δa is

$$\Delta a = \sqrt{\left(\frac{\partial a}{\partial \beta} \Delta \beta\right)^2} \quad (41)$$

Where $\frac{\partial a}{\partial \beta}$ is given by

$$\frac{\partial a}{\partial \beta} = -0.5n\lambda \cot \beta \csc \beta \sqrt{h^2 + k^2 + l^2} \quad (42)$$

so Δa is given by

$$\Delta a = \pm \left| 0.025n\lambda \cot \beta \csc \beta \sqrt{h^2 + k^2 + l^2} \right| \quad (43)$$

as the uncertainty in β is $\pm 0.05°$.

D.2 Error in the Mean

From Gauss' error law, the error due to addition of multiple variables, $z = a_1x_1+a_2x_2+...+a_nx_n$, where a_n is a scalar, is given by

$$\Delta z = \sqrt{(a_1\Delta x_1)^2 + (a_2\Delta x_2)^2 + ... + (a_n\Delta x_n)^2} \tag{44}$$

In the case of a mean, $a_1 = a_2 = ... = a_n = \frac{1}{n}$, meaning the error in the mean value, $\overline{x}$ is given by

$$\Delta\overline{x} = \frac{\sqrt{(\Delta x_1)^2 + (\Delta x_2)^2 + ... + (\Delta x_n)^2}}{n} \tag{45}$$

where

$$\overline{x} = \frac{x_1 + x_2 + ... + x_n}{n} \tag{46}$$

References

[1] J. R. Hook and H. E. Hall, *Solid State Physics*, 2nd ed. Chichester, UK: John Wiley & Sons, 1991.

[2] B. D. Cullity and S. R Stock, *Elements of X-Ray Diffraction*, 3rd ed. New Jeresy, USA: Prentice Hall, 2001.

[3] G. Dolling, H. G. Smith, R. M. Nicklow, P. R. Vijayaraghavan, and M. K. Wilkinson, "Lattice Dynamics of Lithium Fluoride," *Phys. Rev.*, 168, 3, 970-979, Apr 1968. DOI: 10.1103/PhysRev.168.970

[4] "Properties of Solids," in *CRC Handbook of Chemistry and Physics*, 95th ed, W. M. Haynes, Ed. CRC Press, 2016, p.12-80

[5] "Properties of Solids," in *CRC Handbook of Chemistry and Physics*, 95th ed, W. M. Haynes, Ed. CRC Press, 2016, p.12-81

[6] D. K. Bowen and B. K. Tanner, *High Resolution X-ray Diffractometry and Topography*. London, UK: Taylor & Francis Ltd, 1998.

[7] S. Elliott, *The Physics and Chemistry of Solids*. Chichester, UK: John Wiley & Sons, 1997.

[8] C. Kittel, *Introduction to Solid State Physics*, 8th ed. USA: John Wiley & Sons, 2005.

[9] F W C Boswell 1951 Proc. Phys. Soc. A 64 465 Doi: 10.1088/0370-1298/64/5/305